applied sciences

MDPI

Article

Optimizing Extraction of Cellulose and Synthesizing Pharmaceutical Grade Carboxymethyl Sago Cellulose from Malaysian Sago Pulp

Anand Kumar Veeramachineni [1,†], Thenapakiam Sathasivam [2,†], Saravanan Muniyandy [2,*], Pushpamalar Janarthanan [1,†], Steven James Langford [1] and Lim Yau Yan [1]

1 School of Science, Monash University Malaysia, Jalan Lagoon Selatan, Bandar Sunway 47500, Selangor, Malaysia; akvee1@student.monash.edu (A.K.V.); pushpa.janarthanan@monash.edu (P.J.); steven.langford@monash.edu (S.J.L.); lim.yau.yan@monash.edu (L.Y.Y.)

2 School of Pharmacy, Monash University Malaysia, Jalan Lagoon Selatan, Bandar Sunway 47500, Selangor, Malaysia; tsat10@student.monash.edu

* Correspondence: saravanan.muniyandy@monash.edu; Tel.: +603-5514-4926; Fax: +603-5514-6323

† These authors contributed equally to this work.

Academic Editors: Helmut Martin Hügel and Rajender S. Varma
Received: 13 January 2016; Accepted: 25 May 2016; Published: 8 June 2016

Abstract: Sago biomass is an agro-industrial waste produced in large quantities, mainly in the Asia-Pacific region and in particular South-East Asia. This work focuses on using sago biomass to obtain cellulose as the raw material, through chemical processing using acid hydrolysis, alkaline extraction, chlorination and bleaching, finally converting the material to pharmaceutical grade carboxymethyl sago cellulose (CMSC) by carboxymethylation. The cellulose was evaluated using Thermogravimetric Analysis (TGA), Infrared Spectroscopy (FTIR), X-Ray Diffraction (XRD), Differential Scanning Calorimetry (DSC) and Field Emission Scanning Electronic Microscopy (FESEM). The extracted cellulose was analyzed for cellulose composition, and subsequently modified to CMSC with a degree of substitution (DS) 0.6 by typical carboxymethylation reactions. X-ray diffraction analysis indicated that the crystallinity of the sago cellulose was reduced after carboxymethylation. FTIR and NMR studies indicate that the hydroxyl groups of the cellulose fibers were etherified through carboxymethylation to produce CMSC. Further characterization of the cellulose and CMSC were performed using FESEM and DSC. The purity of CMSC was analyzed according to the American Society for Testing and Materials (ASTM) International standards. In this case, acid and alkaline treatments coupled with high-pressure defibrillation were found to be effective in depolymerization and defibrillation of the cellulose fibers. The synthesized CMSC also shows no toxicity in the cell line studies and could be exploited as a pharmaceutical excipient.

Keywords: ecofriendly; sago palm; carboxymethyl; cellulose; pharmaceutical grade; extraction

1. Introduction

The use of natural raw materials for the synthesis of polymers and polymer-based products has been one of the most vital innovations in recent years [1–5]. The use of biomass-based materials has received genuine attention due to their availability, relatively low-cost and favorable sustainability profile [6]. One of the major agricultural waste materials in Malaysia is lignocellulosic biomass from sago starch industries. Lignocellulose contains three main components: an amorphous hemicellulose, a semi-crystalline cellulose and amorphous phenylpropanoid called lignin [7]. The complete and efficient re-use of lignocellulose into usable value-added materials has been a major challenge for both chemical and biological methods. In the overall processes, it is critical to deconstruct the 3D structure

of the lignocellulose by separating the semi-crystalline cellulose and hemicellulose without causing much degradation to the polysaccharide they are formed from [8].

Cellulose has been extracted from different sources [9–12] by different methods, e.g., chemical, mechanical, biological and chemo-mechanical [13–16], but the quality varies widely depending on the source of the cellulose. The most expensive method uses biology, whereas a combination of chemical and mechanical methods shows evidence of producing cheaper and efficient methods of extraction [17]. Native cellulose has a wide range of applications, but it also shows some undesired properties which limit their use. Cellulose has two major polymorphs. In most plants, cellulose I is predominant while cellulose II is found in simpler species like algae allomorphs, in which parallel and antiparallel orientation of the glucan chain is observed. As a material, cellulose exhibits no response to change in pH, solubility in water or other organic solvents. Strong alkali treatment can be employed to alter the crystallinity of cellulose I. Cellulose substituted with alkyl groups, such as methyl, ethyl, hydroxymethyl, hydroxypropyl, and carboxymethyl, produce polymers with variable, and tunable physicochemical properties. Being produced from renewable natural resources has economic gains over synthetic polymers, and, as such, cellulose polymers are utilized in various industries.

One such cellulose derivative is carboxymethyl cellulose (CMC), which possesses strong interactions with metal ions due to the presence of carboxylate and hydroxyl groups. CMC is used in many industries like food, personal care, detergent, mining flotation, paper making, oil drilling and textile industries because of the high viscosity, water preservation, robust acid and salt resistances [18]. There is a recurrent interest in finding cheaper alternative sources for producing CMC, especially since it is widely used at scale in agriculture, forestry, life sciences and chemical communities of United States of America [19].

Methods are available to prepare CMC from natural biomass such as banana plants and sugar beet pulp [20,21]. The synthesis of CMC with hydrogel properties usually involves the reaction of cellulose with sodium monochloroacetate under alkaline conditions [22–24]. We previously reported synthesis and characterization of carboxymethyl sago pulp (CMSP) hydrogels from sago waste [25]. CMSP, is a water-soluble derivative of cellulose that exhibits high solubility [26] and chemical stability, is safe, non-toxic, hydrophilic, as well as biocompatible and biodegradable [27] hence adhering closely to green chemistry principles [26]. In this research, a modified and extraction efficient method to produce cellulose I and carboxymethyl sago cellulose (CMSC) from sago biomass are explored. The purified CMSC was compared to commercial-grade CMC and found to conform to specifications for CMC in the American Society for Testing and Materials (ASTM) standards.

2. Materials and Methods

2.1. Materials

Sago biomass was obtained from Ng Kia Kilang Sagu Industries Sdn. Bhd., Batu Pahat, Johor Bharu, Malaysia. Sodium hydroxide pellets (97%), sodium monochloroacetate (98%), sodium chlorite (80%) technical grade and sodium carboxymethylcellulose (average MW $\approx$ 900,000 g/mol) were obtained from Sigma-Aldrich (St. Louis, MO, USA). Glacial acetic acid (99.9%), acetone (99.6%), isopropanol (99.9%), ethanol (absolute), chloroform, formic acid, hydrogen peroxide (30%) and phenolphthalein obtained from Fisher Scientific (St. Louis, MO, USA).

2.2. Isolation of Alpha Cellulose

Dry sago biomass was ground and passed through a 100 µm sieve [28]. The sieved sago biomass was washed with a 2% non-ionic detergent to remove water-soluble organic compounds and dirt. The residue was then dried at 60 °C for 12 h before being de-waxed using chloroform:ethanol (2:1 v/v) in a Soxhlet extractor for 12 h, followed by 24 h extraction using 96% absolute ethanol. The sago pulp was then oven-dried (60 °C) and the yield of extractive-free lignocellulose biomass determined.

2.2.1. Pulping Method 1

The de-waxed sago pulp was first bleached with sodium chlorite (fiber:hot water:sodium chlorite of 20:640:6 ($w/v/w$)) at pH 4.5 for 3 h at 70 °C to remove the lignin. The pH was adjusted using acetic acid. The white residue obtained was washed with distilled water, then the neutral residue was suspended in 20% (v/v) formic acid and 10% (v/v) hydrogen peroxide solutions at 1:1 ratio and autoclaved at 121 °C and 1.5 bar for 20 min, then washed with 20% formic acid (w/v) and distilled water, to produce holocellulose. The holocellulose was then suspended in 10% of hydrogen peroxide (w/v) at pH 11 and incubated at 80 °C for 30 min. The pH was adjusted with 10% (w/v) sodium hydroxide. The white suspension obtained was filtered and dried at 60 °C to yield cellulose A.

2.2.2. Pulping Method 2

The de-waxed sago pulp was first bleached with sodium chlorite (fiber:hot water:sodium chlorite of 20:640:6 ($w/v/w$)) at pH 4.5 for 3 h at 70 °C to remove lignin. The pH was adjusted using acetic acid. Obtained cellulose was labeled as cellulose B.

2.2.3. Pulping Method 3

De-waxed sago biomass (8% w/v in water) was treated with 90% formic acid (w/v) and 4% hydrogen peroxide (w/v) solutions and heated at 80 °C for 2 h The crude cellulose was bleached using 5% (v/v) hydrogen peroxide at pH 11 for 1.5 h at 80 °C, then filtered, and washed using formic acid and the pH was adjusted to neutral using 10% (w/v) sodium hydroxide. Then the white residue was washed with distilled water and was then dried and labeled as cellulose C.

2.2.4. Pulping Method 4

De-waxed sago biomass (10% w/v in water) was treated with 10% (w/v) hydrogen peroxide and 10% (w/v) sodium hydroxide solutions at 121 °C for 20 min. The crude cellulose was filtered and treated with 20% (v/v) formic acid and 10% (v/v) hydrogen peroxide solutions at 80 °C for 3 h. Then the white residue obtained was then dried and labeled as cellulose D [29].

2.2.5. Pulping Method 5

A similar protocol to pulping method 4 [29] was used followed by the sodium chlorite bleaching treatment from pulping method 2 [30]. The obtained cellulose was labeled as cellulose E.

2.3. Synthesis of CMSC

The carboxymethylation of cellulose to produce CMSC involved three steps: Alkali cellulose formation, carboxymethylation, and purification. The alkali cellulose was produced by adding cellulose (5 g) in isopropanol (100 mL) followed by drop-wise addition of 10 mL of 25% (w/v) sodium hydroxide solution with the resultant mixture stirred at 200 rpm for an hour using an automated stirrer. During alkylation, 3 g of sodium monochloroacetate (MCA) was added to the mixture which was further stirred at 45 °C for 3 h at 200 rpm. The reaction mixture was then cooled and filtered, and the product was suspended in 300 mL of methanol and stirred using a mechanical stirrer for 12 h to remove any undesired impurities. The suspension was then neutralized with glacial acetic acid, and washed three times with 70% (v/v) ethanol and finally with 95% (v/v) ethanol, filtered, and dried at 60 °C till constant weight [25]. Approximately, 5 g of synthesized CMSC was then dissolved in 100 mL of distilled water at 80 °C with constant stirring for 10 min. The mixture was then centrifuged for 1 min at 4000 rpm. The dissolved CMSC was reprecipitated in 100 mL acetone. Recovered CMSC was filtered and washed several times with ethanol and dried at 60 °C until constant weight. The resultant solid was ground and sieved through 150 µm and was kept in a desiccator for characterization.

2.4. Characterization of Cellulose and CMSC

To understand the chemical composition of sago biomass and extracted cellulose, different parameters (Table 1) were determined using the following standard methods.

Table 1. Physicochemical analysis of cellulose.

Methods	Components Analysed
ASTM D 1102-84	ash content
ASTM D 11 11-84	hot water extractives
modified ASTM D 1 107-84	ethanol/toluene extractives
TAPPI 223 cm-84	Pentosan
ASTM D 1106-84	Lignin content
TAPPI T-203 0s-74	α-cellulose
ISO 5351-11998	The viscosity average degree of polymerization of α-cellulose (DPv)

To determine carbohydrate content of the sago cellulose, a quantitative saccharification with sulfuric acid was performed and the resulting monosaccharides were estimated by HPLC (Agilent, 1100 Series). The HPLC system was equipped with a LC-20AT pump, SPD-M20A diode array detector and a Rheodyne injection valve (20 µL loop). The acidic samples were then neutralized using solid Ba(OH) [2] and then the pH was adjusted to pH 6 using saturated aqueous solution of $Ba(OH)_2$. The samples were then filtered through a 0.45 µm filter and analyzed using internal standards (D(+)glucose, D(+)xylose, D(+)galactose, L(+)arabinose, and D(+)mannose). Bio-Rad Aminex HPX-87P column (300 × 7.8 mm) (Bio-Rad, Hercules, CA, USA) at 85 °C was equipped to perform HPLC and distilled H_2O was used as a solvent at flow rate 0.7 mL/min. The injection sample was 20 µL and refractive index detector (RID) at 25 °C was used to detect eluted monosaccharides.

The infrared spectra of all samples were measured between 600 and 4000 cm^{-1} using a Varian 640-IR FTIR spectrophotometer(Varian Medical Systems, Palo Alto, CA, USA) at ambient temperature. Thermal properties of the sago cellulose samples and CMSC were carried out using a thermogravimetric analyzer (Mettler Toledo STARe SYSTEM, Mettler-Toledo, Greifensee, Switzerland). Differential scanning calorimetry (Mettler Toledo DSC 1 STARe System, Mettler-Toledo, Greifensee, Switzerland) was used to analyze the phase transformations of sago cellulose and CMSC samples. Field emission scanning electron microscopy (SU8010) was used to study the shape, size and surface morphology of all the samples. The samples were platinum coated, and an accelerating voltage of 1 kV was used during imaging. The energy dispersive X-ray spectroscopy (EDX) was used for CMSC samples to detect any heavy metal impurities in the samples.

For average molecular weight measurement, cellulose samples were dispersed in NaOH/urea solution and stored at −4 °C for 12 h. The viscosity of cellulose samples were measured at 25 °C using an Ubbelodhe viscometer. To estimate intrinsic viscosity (η), Huggins and Kraemer plots were equipped. Average molecular weight of the cellulose samples was determined using the relation between intrinsic viscosity (η) and viscosity-average molecular weight. The Equation (1) is as follows [31].

$$\eta = 3.85 \times 10^{-2}\ Mw\ 0.76\ \ (mL/g) \quad (1)$$

To understand the fundamental crystallinity and chemical structure of the cellulose samples, X-ray diffraction patterns were acquired for each sample using a D8-Advance Bruker-AXS X-ray diffractometer (Bruker, Billerica, MA, USA) set at 1.540 Å wavelength (CuKα radiation), with a scan speed of 2° per second and a 2θ range of 2° to 30°. Sago cellulose and CMSC samples were analyzed using Bruker Avance 300 (7.05 Tesla magnet) and Bruker Avance III 900 US2 Ultra-High Field NMR magnet system (Bruker, Billerica, MA, USA) (14.1 Tesla magnet) with a 5 mm CPTCI ^{1}H-$^{13}C/^{15}N/D$. The ^{1}H NMR analysis was carried out at 600 MHz whereas ^{13}C spectra were recorded at 150 MHz.

In all cases, samples were dissolved in deuterated water (≈0.5% w/v) and spectra were recorded using HPDEC (high-power decoupled) techniques.

2.5. Physical Characterization of CMSC

2.5.1. Determination of Degree of Substitution (DS)

Absolute values of the DS of CMSC products were determined by the standard method (ASTM D1439, West Conshohocken, PA, USA). In this method, 4 g of the dry powder CMSC was stirred in 75 mL of 95% ethanol for 5 min. Then 5 mL of 2 M nitric acid was added and the solution was boiled to convert NaCMSC to its acid form, H-CMSC. Next, the solution was removed from the heat and further stirred for 10 min. The liquid phase was removed, and the solid phase was washed with 20 mL of 80% (v/v) aqueous ethanol solution at 60 °C. The ethanol washing was repeated for four times. The precipitate was then washed with a small quantity of anhydrous methanol and filtered. Finally, the precipitate was dried at 100 °C for 3 h and cooled in a desiccator for half an hour.

About 0.5 g of dry acid CMSC was weighed, and 100 mL of distilled water was added and stirred. Then 25 mL of 0.3 M NaOH was added and the mixture was heated to boil for 15 min. After complete solubilization of CMSC, the solution was titrated with 0.3 M HCl using phenolphthalein as indicator. The titration was repeated thrice for each sample, and the average volume of HCl used was recorded. The degree of substitution was then calculated using Equations (2) and (3) as follows:

$$Carboxymethyl\ content\ \ (\%CM) = [(Vo - Vn)\,N \times 0.058 \times 100]\,/M \tag{2}$$

$$Degree\ of\ substitution = 162 \times \%CM/\,[5800 - (57 \times \%CM)] \tag{3}$$

where V_o = mL of HCl used to titrate blank, V_n = mL HCl used to titrate sample, N = normality of HCl used, M = sample amount (g), and 58 = molecular weight of carboxymethyl group [28].

2.5.2. Determination of Moisture Content

The moisture content of the CMSC was determined according to ASTM D 1439-03. About 3 g of the sample was placed in an open sample bottle and heated in an oven at 105 °C for 2 h. The sample was then cooled, and the bottle was closed and weighed. The sample was then replaced in the oven for 30 min, cooled and reweighed. This procedure was continued until the mass loss was not more than 5 mg for 30 min drying time. The percent moisture, M, was calculated using Equation (4) as follows:

$$M = \left(\frac{A}{B}\right) \times 100 \tag{4}$$

where:

A = Mass loss on heating, g
B = sample used, g

2.5.3. Determination of Solubility and pH

Quantitative solubility tests were carried out in 3% (w/v) CMSC in water. The pH was measured using a pH meter (Mettler-Toledo S20; Mettler-Toledo, Greifensee, Switzerland). The mixture was stirred at room temperature for 16 h to obtain a uniform suspension. The sample was then centrifuged for 10 min at 1500 rpm. After centrifugation, 25 mL of clear supernatant was transferred by pipette into a dry pre-weighed sample bottle. The weighing bottle was dried at 105 °C in an oven until constant weight (approx. 24 h). It was then cooled in a desiccator and weighed. The solubility was calculated using Equation (5) as follows:

$$\text{The solubility of sample in 3\% } (w/v) \text{ aqueous solution } = \frac{W_d \times 100}{25 \times 0.03} \tag{5}$$

where:

W_d = weight of dried soluble sample in 25 mL

2.5.4. Determination of Average Molecular Weight

Static light scattering experiments were performed with a multiangle photometer equipped with a He-Ne laser (λ = 661.0 nm) (DAWN-HELEOS, Wyatt Technology Corporation, Goleta, CA, USA). The scattered light intensities were recorded in an angular region from 30° to 150° at a temperature of 25.0 ± 0.1 °C. Test solutions were made optically clean by filtration through 0.2 µm Millipore filters (Merck & Co., Inc., Kenilworth, NJ, USA) directly into a clean vial for light scattering measurements. Astra 6 software was used to collect the signal and analyze the data (Wyatt Technology Corporation, Goleta, CA, USA). The refractive-index (RI) increment values, dn/dc, used is 0.150 mL/g and the flow rate is 1.000 mL/min. Fused silica cell and the RI increment is analysed by Optilab rEX and the solvent used is 0.1 M $NaNO_3$ with 0.5 g/L NaN_3.

2.6. Determination of Heavy Metals and Other Physicochemical Parameters

The presence of heavy metals in the samples was analyzed using ICP-MS (ICPMS 7500 Single Turbo System, Agilent, Santa Clara, CA, USA). Color measurement was conducted using tristimulus colorimeter (HunterLab ColorFlex, Hunter Associates Laboratory Inc., Reston, VA, USA) according to ISO 2470:1999. Tapped density (ETD-1020, Electrolab India Pvt. Ltd., Navi Mumbai, India) measurements were conducted according to United States Pharmacopeia, 2010.

2.7. Cytotoxicity and Biocompatibility of CMSC

Human cervical carcinoma (HeLa) cells were used in a cell suspension containing 1×10^5 cells mL^{-1}. The cells were seeded into each well of 96-well tissue culture plates and incubated for 18 h followed by addition of CMSC at concentrations of 100–1000 µg/mL and further incubated for 48 h at 37 °C. Then, yellow tetrazolium MTT (3-(4,5-dimethylthiazolyl-2)-2,5-diphenyltetrazolium bromide) (10 µL; 5 mg·mL^{-1}) (MTT Assay kit, Nacalai Tesque, Japan) was added and the optical density (OD) value at 570 nm of each well, with background subtraction at 690 nm, was measured by means of a microtitre plate reader. The following formula was used to calculate the inhibition of cell growth; all assay experiments were performed in triplicate for each sample was calculated using Equation (6) as follows:

$$\text{Cell viability } (\%) = \frac{\text{mean of abs. value of treatment group}}{\text{mean absorbance value of control}} \times 100 \quad (6)$$

Direct contact tests were conducted to investigate the biocompatibility of CMSC samples according to ASTM F-813-83 (ASTM, 1983) and ISO 10993-5 (ISO/EN, 1992) with slight modification. The cells were examined by light microscopy (EVOS, AMG, Washington, WA, USA) [32].

3. Results and Discussion

3.1. Sago Biomass and Cellulose Composition

The composition of sago biomass is given in Table 2. The major components were found to be holocellulose (55% w/w), and an equal amount of lignin and ash (8% w/w of each component). Simple sugars, such as arabinan (6% w/w) and xylan (3% w/w), were also obtained. The extracted cellulose samples were subjected to standard methods to estimate the percentage of lignin, alpha cellulose, intrinsic viscosity, ISO brightness, crystallinity and total yield of cellulose. As shown in Table 3, pulping method 1 exhibits higher crystallinity (63%), brightness (~95) and alpha cellulose (~94%) with least lignin (0.56%) content compared to material obtained from methods 2 to 5. The average molecular weight of cellulose obtained from method 1 is approximately 55,000 g/mol.

Table 2. Chemical composition of sago biomass.

Fraction	% Dry Sago Biomass (% DSB)
Ash	8.00
Ethanol toluene extractives	2.30
Hot water extractives	5.20
Xylan (HPLC)	5.98
Arabinan (HPLC)	3.10
Klason lignin	8.10
Chlorite holocellulose	55.10
α-cellulose	33.70

Table 3. Chemical composition, physical and chemical properties of cellulose extracted by different methods.

Cellulose Composition	Standard Method	Method 1	Method 2	Method 3	Method 4	Method 5
Lignin (%)	TAPPI T 15 os-80 oos-80	0.56	5.20	4.58	10.26	3.60
α-Cellulose (%) (%)	TAPPI T203 om-93	93.60	70.40	90.80	92.60	87.80
ISO brightness	ISO 3688-1999	94.61	90.10	86.85	88.77	80.03
Intrinsic Viscosity (mL/g)	Viscosity measurement	1400–1650	525–600	600–850	550–610	700
Crystallinity(2θ)	X-ray diffraction	0.63	0.59	0.64	0.63	0.45
Total yield of cellulose %	HPLC	5.38	10.17	7.09	3.53	8.80

3.2. Fourier Transform Infrared Spectroscopy Studies

The following explanation of Figure 1 refers to the consistent features of spectra A–I. The spectra in Figure 1 show a strong, broad peak at 3200–3600 cm^{-1}, attributable to an O–H stretching vibration consistent with the polyhydroxylated saccharide backbone, and a weak absorption band at 2887–2933 cm^{-1} consistent with the C-H stretching within each glucose unit [33]. A strong band is appearing at 1423–1433 cm^{-1} indicates the alkane deformations relating to CH and CH_2 [34]. The peak appearing in the 1330–1369 cm^{-1} region of the spectra attributes to the in-plane bending vibration of the C-H and C-O groups of the hexose ring in the cellulose. A similar band was also seen in the nano-cellulose isolated from sugarcane waste [35]. The peaks at 1051–1059 and 779–809 cm^{-1} are associated with the C-O stretching and C-H rocking vibration [36] (anomeric vibration, specific for glucosides) [37]. The peak at about 900 cm^{-1} is related to glycosidic –C1-H deformation, a ring vibration, and –O–H bending where these characters infer the β-glycosidic linkages between anhydroglucose units [38]. The increase in peak intensity at 1018 cm^{-1} reveals that the cellulose content of the material increases as a result of the various chemical treatments. The absorption peaks around 3400, 2900, 1430, 1370, 890 cm^{-1} are associated with the characteristics [39] of native cellulose I as seen in all cellulose spectra. The appearance of a peak at around 1645 cm^{-1} in all samples indicates absorption of water by cellulose and CMSC. This peak is related to the bending modes of water molecules due to its strong interaction with cellulose backbone [40]. The peak intensity at 1514 cm^{-1} in Figure 1 from cellulose (E–H) attributes to the C=C stretching vibration in the aromatic skeletal vibration in lignin. However, cellulose (B) did not show the C=C stretching in that region. It indicates that lignin was removed due to the combined processes of delignification and acidified sodium chlorite process. Cellulose (E) also shows a peak at 1724 cm^{-1} that represent the ester linkage of the carboxylic group of ferulic and *p*-coumaric acids in hemicelluloses. The absence of this peak in cellulose (A, C, D, E) would indicate the removal of the hemicellulose during the chemical treatment. Figure 1A,D shows similar peaks stating that commercial cellulose and cellulose A (preparation method 1) are chemically similar and, therefore, the hydrolysis reaction performed did not affect the chemical structure of the cellulosic fragments [41]. However, the peaks in cellulose (E) are not identical to (A). This, therefore, indicates that cellulose (A) prepared by method 1 is ideal to synthesize CMSC. In Figure 1I the proof of carboxymethylation in CMSC is observed where a strong absorption band appeared at 1589 and 1020 cm^{-1}, which indicates the presence of carboxymethyl groups [42].

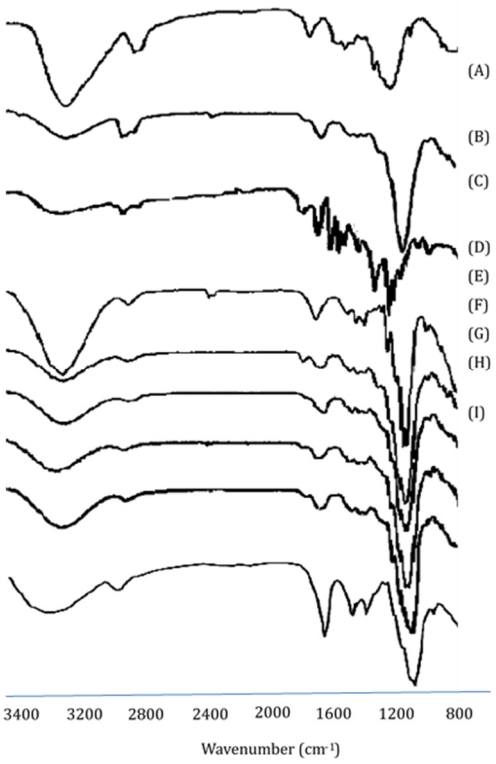

Figure 1. FTIR (Infrared Spectroscopy) spectra of commercial cellulose (**A**); sago biomass (**B**); commercial lignin (**C**); cellulose A (preparation 1) (**D**); cellulose B (preparation 2) (**E**); cellulose C (preparation 3) (**F**); cellulose D (preparation 4) (**G**); cellulose E (preparation 5) (**H**) and carboxymethyl sago cellulose (CMSC) (**I**).

3.3. Thermogravimetric Analysis

Figure 2 indicates the thermogravimetric analysis of all cellulose preparations and CMSC. All samples exhibit a small weight loss in the low-temperature range (<100 °C), corresponding to the evaporation of absorbed water [43]. The weight loss rate was within 12% to 13% of the total weight. Cellulose B (Figure 2D) shows an earlier weight loss that begins at 200 °C and reached a dominant peak at 370 °C. This is due to the presence of hemicellulose that decomposes easily, and has weight loss between 200 and 300 °C [44] which were not seen for cellulose A, C, D, and E. The maximum weight loss rate (0.8 wt %/°C) occurred at 350–400 °C, which took place for all samples where cellulose was seen to decompose, providing mainly volatile products. Due to the complex composition and structure of lignin, the decomposition process is slower and covers a wide range of temperature than cellulose and hemicellulose. The decomposition shows broad and flat peaks with a gently sloping baseline, which heightens the difficulty in defining the activation energy for the reaction. This is where cellulose stands out from hemicellulose as it shows a sharper thermal analysis peak, inducing a definite tailing section at a higher temperature. When the temperature was greater than 400 °C, almost all cellulose was pyrolyzed with a very low solid residue (0.1 wt %/°C) left. Lignin decomposition happened slowly over the whole temperature range [45] and the solid residue left from lignin are about ~46 wt %. The conversion of cellulose to CMSC through chemical reaction affects both the molecular structure and bonding energy of the material, resulting in the different thermal behavior of CMSC [46]. Figure 2H shows the derivatograms of CMSC where the highest weight loss occurs at 310 °C, and this is due to the loss of CO_2 from carboxymethyl groups of CMSC [47]. The degradation temperature of CMSC decreases as compared to cellulose due to the presence of sodium. This is due to the interference with crystallinity as the presence of random irregularities produced by the relatively bulky side groups of carboxymethyl substituted on the cellulose backbone [48]. Replacing the hydroxyl

group of cellulose by -O–Na^+ leads to the swelling of the molecule, thereby increasing its reactivity towards carboxymethylating agent to form CMSC. Hence, the migration of Na^+ into the cellulose lattice planes disrupts the hydrogen bonded crystalline region and, therefore, weakens the energy bonding of cellulose, which results in reduced stability of CMSC to heat.

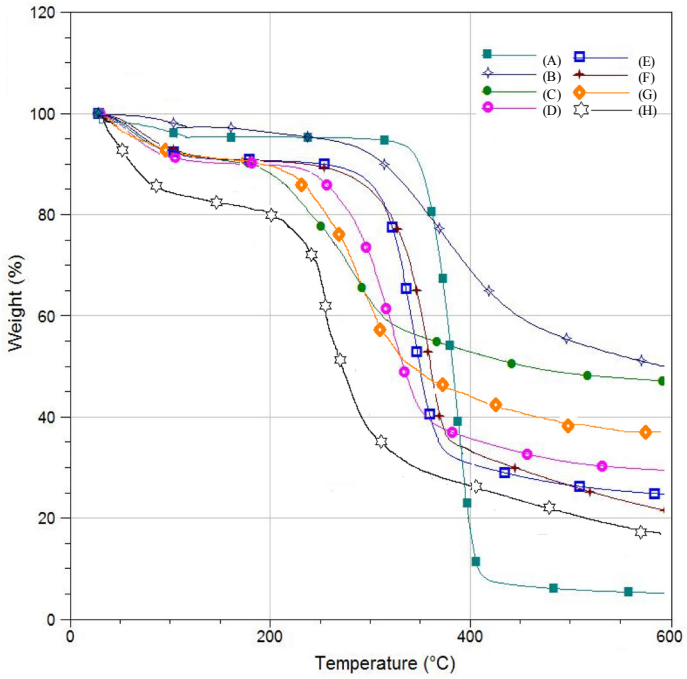

Figure 2. TGA (Thermogravimetric Analysis) of commercial cellulose (**A**); commercial lignin (**B**), cellulose A (preparation 1) (**C**); cellulose B (preparation 2) (**D**); cellulose C (preparation 3) (**E**); cellulose D (preparation 4) (**F**); cellulose E (preparation 5) (**G**); and CMSC (**H**).

3.4. Differential Scanning Calorimetry

Figure 3 shows DSC curve that indicates the energy consumption property of cellulose and CMSC samples. The DSC thermogram exhibits an early endothermic peak with an enthalpy change observed at 90–110 °C for all samples. This minor enthalpy change is attributed to desorption of moisture as water trapped in the polysaccharide structure is released. The DSC profile of cellulose B shows an endothermic peak at 250 °C due to non-cellulosic constituents such as hemicellulose [13]. As the temperature increases further, the DSC profile for all cellulose samples shows an endothermic peak at around 350–360 °C. However, cellulose A showed the most prominent endothermic peak at about 355 °C. This could be due to the increase in compactness of the crystallinity structure and involves the breakdown of intramolecular interaction and the decomposition of the cellulose [49]. The major enthalpy change for CMSC (F) occurs at 310 °C exhibiting exothermic peak due to the degradation of cellulose with the carboxylate functional groups. The thermal scission of the carboxylate groups resulted in the evolution of CO_2 from the corresponding cellulose backbone, and this could be a probable thermal mechanism for CMSC thermal transitions.

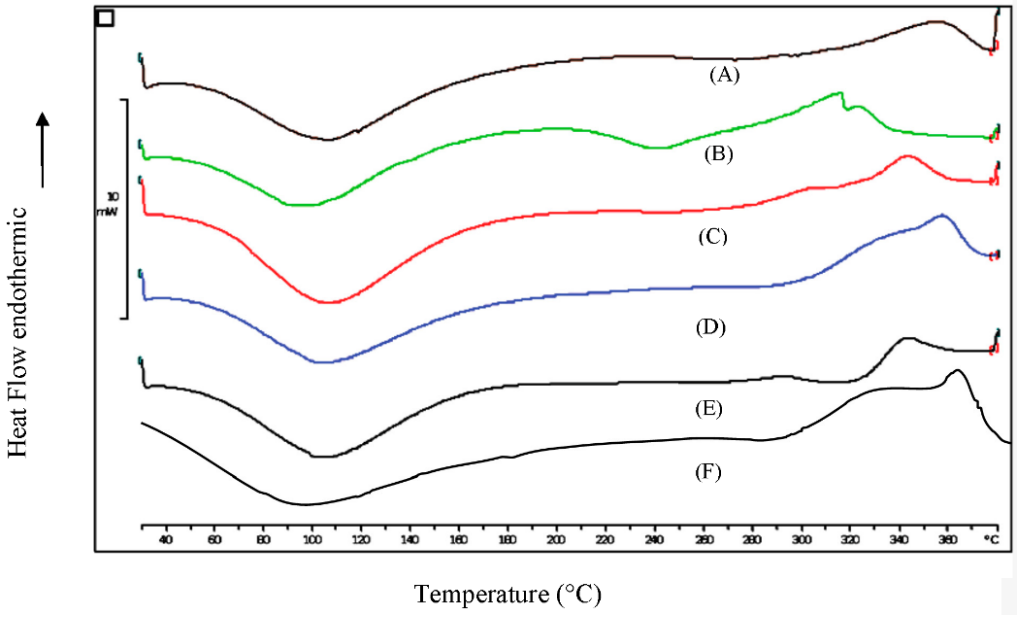

Figure 3. DSC (Differential Scanning Calorimetry) thermogram of cellulose A (preparation 1) (**A**); cellulose B (preparation 2) (**B**); cellulose C (preparation 3) (**C**); cellulose D (preparation 4) (**D**); cellulose E (preparation 5) (**E**); and CMSC (**F**).

3.5. X-Ray Diffraction

The X-ray diffraction (XRD) patterns of natural lignocellulosic fibers displays a typical crystal lattice of cellulose type I, with the main diffraction signals at 2θ values of 15°, 16°, 22.5° and 34° [50] for all cellulose preparations (Figure 4) consistent with cellulose I. The absence of doublet in the main peak at 2θ = 23° indicates the absence of any cellulose II [51]. This indicates that the cellulose structure did not endure any morphological change by chemical treatment, and most of the crystallinity is observed. The sharpness for the diffraction peak at 23° for all cellulose I forms indicates an increase in crystallinity. Sample (A) from Figure 4 shows the highest crystallinity. The increase of crystallinity could be due to the removal of hemicellulose and lignin, which exist in amorphous regions, leading to the realignment of cellulose molecules. Furthermore, during the hydrolysis process, the hydrophilic ions could penetrate into the amorphous regions of cellulose causing hydrolytic cleavage of glycogenic bonds and release of the crystallites [52]. The decrease in the crystallinity could also be due to the breakage of hydrogen bonds in the crystalline part of cellulose chains during pulp treatment. The overall resolution of CMSC peaks indicates an amorphous region rather than highly crystalline region after the carboxymethylation process as expected. This is due to the breakage of inter- and intra-molecular hydrogen bonds in the crystalline part of the cellulose together with an increase in the electrostatic interactions between the CMSC as a result of the anionic $–CH_2COO^-$ groups substituted with the hydroxyl groups of cellulose [30]. A shifting of peaks of 002, 101 in 2θ degree occurred and this could be due to the broadening the distance between cellulose polymer molecules. As the obtained cellulose was solubilized in isopropanol, an organic solvent and also swelling the cellulose in the concentrated sodium hydroxide during carboxymethylation process could have caused the conversion of polymorphs cellulose I to polymorphs cellulose II. Thus, the substitution of carboxymethyl group to the backbone of cellulose leads to the transformation of polymorphs cellulose I in cellulose to polymorphs of cellulose II in CMSC [22].

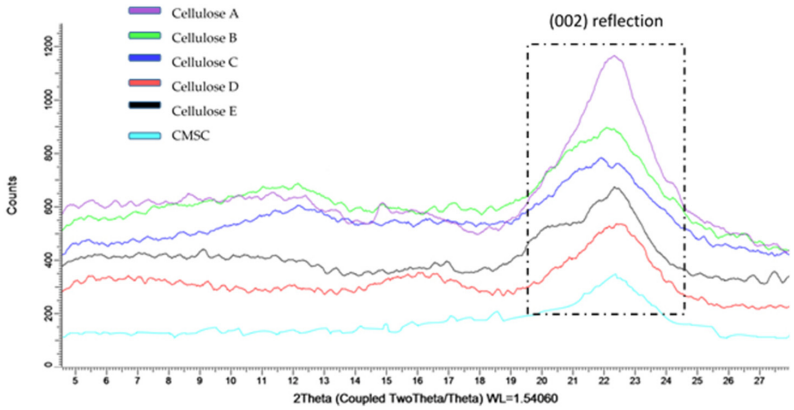

Figure 4. X-ray diffractograms of cellulose A (preparation 1) (**A**); cellulose B (preparation 2) (**B**); cellulose C (preparation 3) (**C**); cellulose D (preparation 4) (**D**); cellulose E (preparation 5) (**E**); CMSC (**F**).

3.6. FESEM

Figure 5 illustrates the surface morphology of extracted celluloses and CMSC. The extracted cellulose samples clearly show unique cellulose structure. The presence of a smooth surface indicates the possibility of hemicellulose and lignin present in the amorphous state (Figure 5B–E). In Figure 5A, it is observed that the sample exhibits the compact structure of fibrils, and the surface roughness is higher due to the crystallinity and rigidity. The appearance in CMSC sample exhibits a very different surface morphology where it is more granular than cellulose. It clearly indicates smooth particles, that are clumped up together due moisture trapped within the particles.

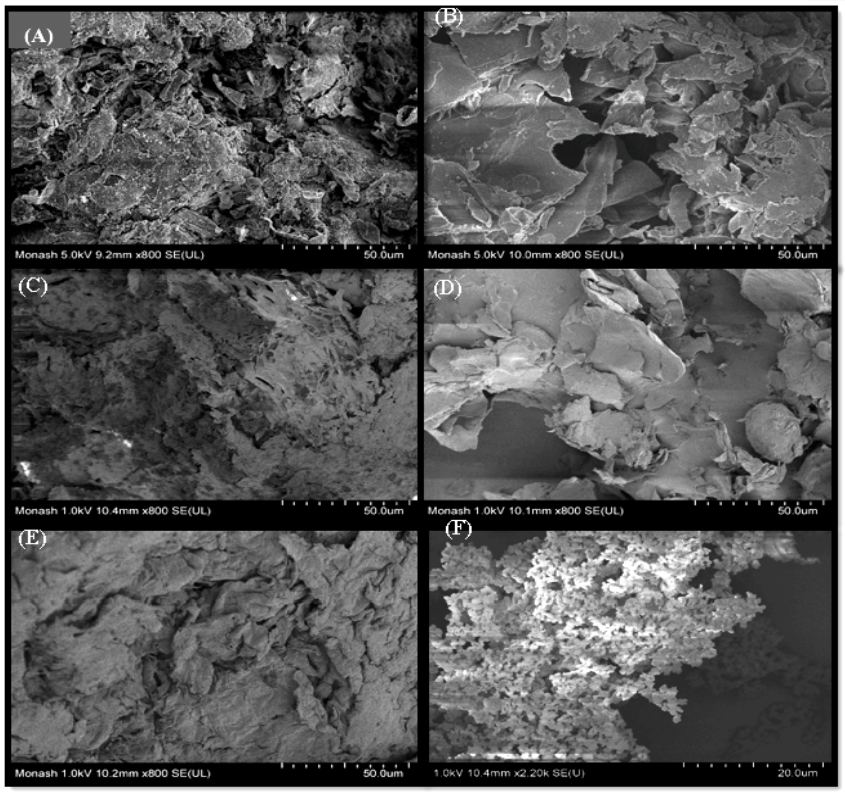

Figure 5. FE-SEM images of cellulose A (preparation 1) (**A**); cellulose B (preparation 2) (**B**); cellulose C (preparation 3) (**C**); cellulose D (preparation 4) (**D**); cellulose E (preparation 5) (**E**); and carboxymethyl sago cellulose (CMSC) (**F**). All cellulose preparation was at ×800 magnification and CMSC was at 2200× magnification.

3.7. NMR

The structure of CMSC is shown in Figure 6Ai. The ^{1}H-NMR spectrum of CMSC (Figure 6Aii) exhibits peak between δ = 3 ppm and 4 ppm were assigned to H 2, H 1 of the glucose subunit. The peaks at positions δ = 4 ppm and 4.5 ppm corresponded to the H 3–6 in the cellulose backbone, respectively. The peaks between δ = 3.88 ppm and 4.41 ppm at position H represent protons of methylene from carboxyl groups. The ^{1}H-NMR spectrum confirms the carboxymethyl sago cellulose was synthesized. The ^{13}C–NMR spectrum of CMSC is seen in Figure 6Aiii with a range between 179 and 59 ppm. A prominent peak at 178 ppm is assigned to the CO carbon (C-8) of the carboxymethyl group. At 96 ppm, it is assigned to C-2 whereas, at 80 ppm, this peak is assigned to C-4. C-2 and C-3 are at 71 and 73 ppm, respectively. As for C-5, the signal appears at 73 ppm. The electron withdrawing effect imposed by oxygen in the carboxymethyl substituent, C-6s (68 ppm) causes a downfield shift of ~7.4 ppm compared to C-6 (61 ppm). The C-7 represents the methylene carbon atoms of the carboxymethyl group appear at three major peaks (71, 70, 69 ppm) as carboxymethyl substitution would take place in three different positions [53].

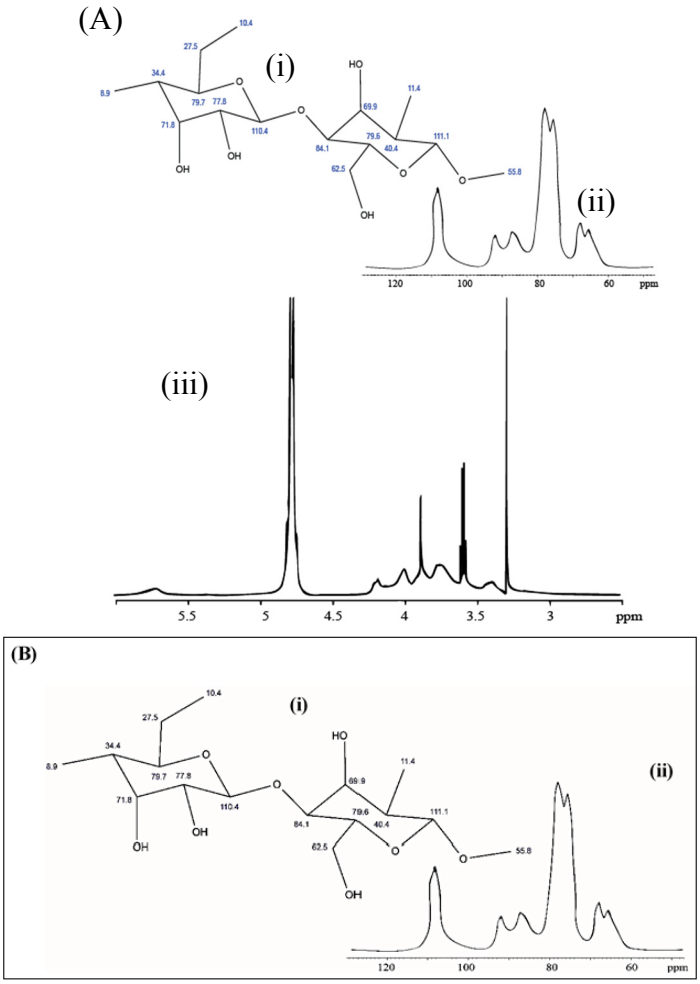

Figure 6. (**A**) (**i**) CMSC structure; (**ii**) ^{1}H-NMR and (**iii**) ^{13}C-NMR spectra of CMSC (DS = 0.6) in D_2O (**iv**) Contour plots of COSY spectra of CMSC (DS = 0.6) in D_2O recorded at 343 K. and (**B**) (**i**) cellulose structure; (**ii**) ^{13}C-NMR spectra of cellulose.

For cellulosic carbon (Figure 6Bi), the ^{13}C-NMR spectrum Figure 6Bii illustrates six singlets corresponding to ^{13}C chemical shifts of cellulose carbons, C1 (105 ppm), C4 (83–97 ppm), C2/C3/C5 (72–80 ppm), and C6 (62–69 ppm) of the anhydroglucose units of cellulose [54]. To determine the

cellulose crystallinity, C4 resonance region is most likely to be used [55]. The changes of specific hydrogen bonding with hydroxyl groups in adjacent cellulose chains would reflect the changes of C6 resonance region. Broad shoulder signals that occur at 83 ppm (C4 region) whereas 63 ppm (C6 region) indicate the presence of amorphous cellulose [56], which could be attributed to the presence of hemicellulose and lignin as they appear amorphous in nature. However, cellulose in Figure 6Bii indicates sharp signals at 84 ppm and 63 ppm, which, respectively, show the existence of crystalline cellulose. A strong signal from 56 ppm reciprocates to aromatic methoxyl (–OCH_3) resonance in lignin [57]. This peak does not appear in the cellulose spectrum indicating the absence of lignin.

3.8. Physical Characterization of CMSC

3.8.1. Degree of Substitution (DS)

The DS is a major factor governing properties such as water solubility of Na-CMC, but below DS 0.4 the polymer is water-swellable and insoluble. The polymer is entirely aqueous soluble with its hydro affinity increasing with increasing DS [58]. An average DS of 0.62 was obtained with isopropanol as the solvent medium. The role of the solvent in the carboxymethylation reaction is to provide accessibility of the etherifying reagent to the reaction centers of the cellulose chain [59]. A NaOH concentration (25%) was utilized according to Pushpamalar *et al.* [30]. This is because, in the carboxymethylation procedure, two competitive reactions take place simultaneously. The first reaction involves sago cellulose hydroxyl groups react with Na-MCA in the presence of NaOH to give CMSC. The second reaction of Na-MCA with NaOH to give sodium glycolate as a byproduct [60]. Hence, increasing the concentration of NaOH could cause the second reaction to prevailing more than the first. According to Pushpamalar *et al.* [25], increasing NaOH would lead to more glycolate formation. Similar research was done on maize starch where it was concluded DS value would also gradually decline due to the sodium glycolate formation in the synthesis of CMC and polymer degradation would also occur due to the high concentration of NaOH [61].

3.8.2. Moisture Content

CMSC showed the ability to absorb moisture from the air, where the amount of moisture absorbed and the rate of absorption is dependent upon the initial moisture content of CMSC. The moisture content of CMSC was approximately 8.11% (*w*/*w*). An explanation is that in the case of CMSC, water is more tightly bound within the superstructure and not so easily dehydrated under the conditions used (oven, 105 °C, 2 h). This tight association may be due to interactions between water molecules and ionic groups with counter-ions or hydroxyl groups functioning as sorption sites for the water molecules.

3.8.3. Molecular Weight, Solubility, and pH

Table 4 indicates the molecular weight (MW) of CMSC, which is 6.296×10^4 g/mol. It is known that the molecular weight would increase due to the number of –OCH_2COONa groups per glucose unit that also increase the hydrodynamic volume of CMSC. This was shown in another study done by Nomura *et al.* [62] regarding about viscosity of CMC and carboxymethylation of dextran [63].

Table 4. Characterization of physical and chemical properties of CMSC (carboxymethyl sago cellulose).

Sample	Degree of Substitution (DS)	Moisture Content (%)	pH	NaOH Content (%)	Tapped Density/g/mL	Solubility/%	Molar Mass (M_w)/($\times 10^4$) g/mol
1	0.59 ± 0.01	8.23 ± 0.94	9.76	1.36 ± 0.21	11.02	93.06	5.8
2	0.61 ± 0.03	7.78 ± 0.66	9.63	1.43± 0.25	11.50	94.45	6.7
3	0.63 ± 0.02	8.32 ± 0.77	9.70	1.27± 0.27	12.12	94.34	6.2
Average	0.61 ± 0.02	8.11 ± 0.79	9.70	1.35 ± 0.24	11.55	93.95	6.2

* Each sample represents average of 3 determinations (n = 3).

In Table 4, the solubility of CMSC is high (95% dissolved) is attributable to the carboxylate group appended to the cellulose backbone [64]. The pH value of the CMSC solution under the conditions tested is 9.7. The elevated alkaline pH value could be due to the presence of a certain amount of NaOH that could have been trapped in the swollen molecules of CMSC even after prolonged washing.

3.9. Limit Test for Heavy Metals and other Physicochemical Parameters

Metal contamination may be introduced in many ways from raw materials since CMSC is synthesized from plant biomass. Therefore, ICP-MS analysis is prescribed by United States Pharmacopoeia (USP), European Pharmacopoeia (EP), and British Pharmacopoeia (BP) to evaluate heavy metal content (limit test). According to Table 5, only elements such as Na, Mg, Al, K and Ca were found in the sample. However, other toxic heavy metal contaminants, such as lead, mercury, arsenic and cadmium (not shown in data), were not found in the sample, indicating that CMSC can be used as a pharmaceutical excipient. The density of CMSC was found to be 11.55 g/mL (Table 4). Color measurement was carried out to determine the color formation that is known to be caused by a reaction in carboxymethylation. The color of CMSC is white as compared to commercial CMC, which was light brown and the total color difference was 0.1053 abs (Table 6). The CMSC color appearance could be due to reprecipitation with acetone.

Table 5. Elements present in CMSC.

Sample	Concentration of Na (ppb)	Concentration of Al (ppb)	Concentration of Mg (ppb)	Concentration of K (ppb)	Concentration of Ca (ppb)
Average	14,540.00 ± 141.42	12.35 ± 6.81	18.08 ± 12.78	1125.80 ± 212.41	25.70 ± 3.42

* Each sample represents average of 3 determinations ± s.d.

Table 6. Color of CMSC DS 0.6.

Sample	Average Value						
	L_0 *	a_0 *	b_0 *	L *	a *	b *	ΔE
1	-	-	-	89.40	0.93	13.30	0.1068
2	-	-	-	89.43	0.94	13.22	0.1581
3	-	-	-	89.43	0.93	13.37	0.0510
Commercial CMC	89.48	0.94	13.37	-	-	-	-
						Average	**0.1053**

* Each sample represents average of 3 determinations (n = 3).

3.10. Cytotoxicity and Biocompatibility

Figure 7A shows the results of the MTT assay and cell morphology observations, which indicate that CMSC had little toxicity in HeLa cells with all concentrations tested. The morphology of HeLa cells was not affected by treatment with CMSC and, therefore, cell proliferation was not inhibited by the CMSC synthesized. The biocompatibility of the CMSC was seen in Figure 7B where the HEK (Human Embryonic Kidney)-Neuroblastoma cells were cultured for 48 h and observed. The morphology of the cells was not affected when compared with positive controls either. The negative control was used as a reference for morphological changes in the cells in the presence of a toxic substance. This indicates that cell proliferation in the presence of CMSC proves that it is bio-nontoxic as it did not negatively influence cellular growth showing a promising potential application as a biomaterial.

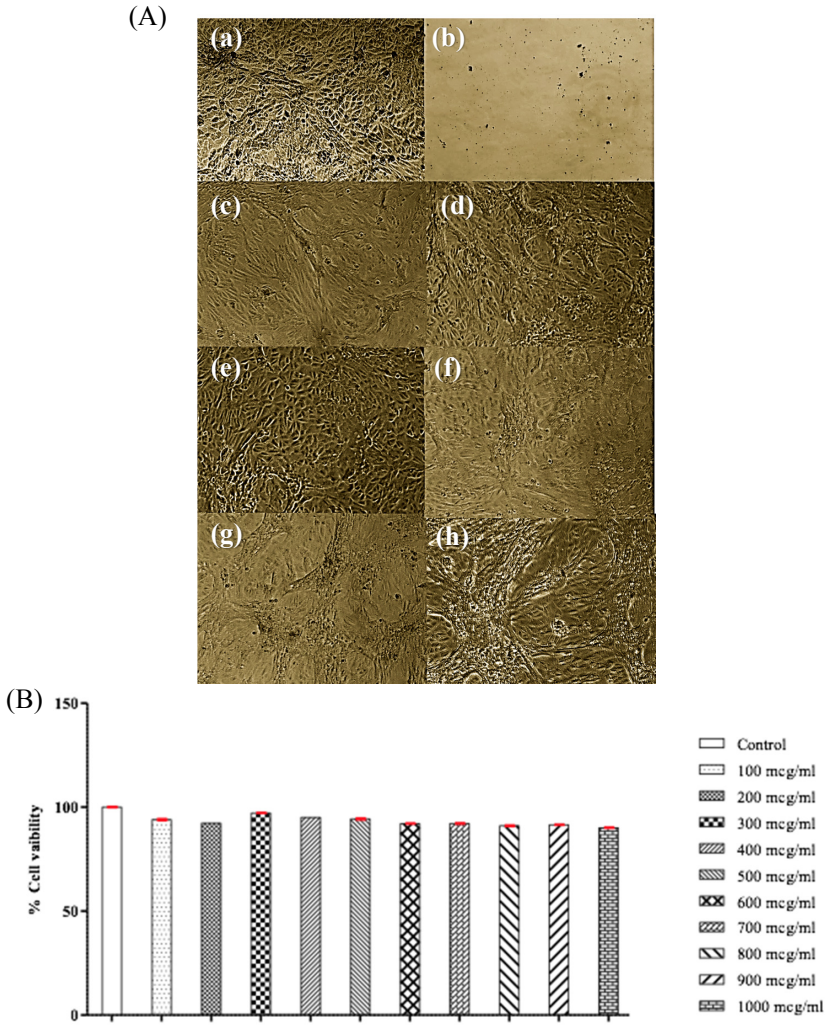

Figure 7. (**A**) Micrographs of HEK (Human Embryonic Kidney) cells cultured in presence of CMSC (**a**); Positive control (**b**); Negative control (cytotoxic 5-Fluorouracil) (**c**) 20 µg of CMSC (**d**) 50 µg of CMSC (**e**) 100 µg of CMSC (**f**) 250 µg of CMSC (**g**) 500 µg of CMSC (**h**) 1000 µg of CMSC; (**B**) Bar graph comparing the cell viability of Hela cells that had been cultured on various CMSC concentration (100–1000 µg/mL).

4. Conclusions

Extraction of cellulose from sago biomass using five different chemical and chemi-mechanical methods were carried out. When considering the chemical composition and microscopic observation, cellulose exhibits high crystallinity and purity. Cellulose extracted from pulping method 1 has proved to be the best cellulose extraction method from sago biomass. Furthermore, this cellulose was subsequently modified to CMSC of DS 0.6. There was a complete loss of crystallinity in CMSC when compared with cellulose and the NMR results confirm that there was expected change in chemical structure as required. The synthesized CMSC is free from heavy metals and toxic substances. The cells cultured on the CMSC samples suggested the biocompatibility of the sample. Considering the aforementioned properties, CMSC has potential a potential application as a pharmaceutical excipient. The developed method could be used to convert sago waste into a value-added product of commercial importance.

Acknowledgments: The synthesis and characterization of purified cellulose and CMSC were funded by the Ministry of Higher Education through Fundamental Research Grant Scheme (FRGS) (FRGS/2/2013/SG06/MUSM/02/1). The article-processing charges are also supported by the FRGS grant. The research work carried at School of Pharmacy and School of Science, Monash University, Malaysia.

Author Contributions: Pushpamalar Janarthanan and Steven James Langford have contributed to the synthesis and the characterization of CMSC from sago biomass; Anand Kumar Veeramachineni and Thenapakiam Sathasivam conducted all the experiments and analyzed the results, Saravanan Muniyandy, and Lim Yau Yan have contributed to pharmaceutical characterization and written the manuscript.

Conflicts of Interest: The authors declare no conflict of interest.

References

1. Siracusa, V.; Rocculi, P.; Romani, S.; Dalla Rosa, M. Biodegradable polymers for food packaging: A review. *Trends Food Sci. Technol.* **2008**, *19*, 634–643. [CrossRef]
2. Mathers, R.T.; Meier, M.A. *Green Polymerization Methods: Renewable Starting Materials, Catalysis and Waste Reduction*; John Wiley & Sons: Hoboken, NJ, USA, 2011.
3. Rodionova, G.; Lenes, M.; Eriksen, Ø.; Gregersen, Ø. Surface chemical modification of microfibrillated cellulose: Improvement of barrier properties for packaging applications. *Cellulose* **2011**, *18*, 127–134. [CrossRef]
4. Ilevbare, G.A.; Liu, H.; Edgar, K.J.; Taylor, L.S. Inhibition of solution crystal growth of ritonavir by cellulose polymers–factors influencing polymer effectiveness. *CrystEngComm* **2012**, *14*, 6503–6514. [CrossRef]
5. Siqueira, G.; Bras, J.; Dufresne, A. Cellulosic bionanocomposites: A review of preparation, properties and applications. *Polymers* **2010**, *2*, 728–765. [CrossRef]
6. Bing, L.; Zhang, Z.; Deng, K. Efficient one-pot synthesis of 5-(ethoxymethyl) furfural from fructose catalyzed by a novel solid catalyst. *Ind. Eng. Chem. Res.* **2012**, *51*, 15331–15336. [CrossRef]
7. Ge, W.; Wang, X. Application of ionic liquids in lignocellulose biomass dissolution, fraction and chemical modification. *Int. J. Condens. Matter Adv. Mater. Supercond. Res.* **2014**, *13*, 369–390.
8. Cox, B.J.; Ekerdt, J.G. Pretreatment of yellow pine in an acidic ionic liquid: Extraction of hemicellulose and lignin to facilitate enzymatic digestion. *Bioresour. Technol.* **2013**, *134*, 59–65. [CrossRef] [PubMed]
9. Li, R.; Fei, J.; Cai, Y.; Li, Y.; Feng, J.; Yao, J. Cellulose whiskers extracted from mulberry: A novel biomass production. *Carbohydr. Polym.* **2009**, *76*, 94–99. [CrossRef]
10. Revol, J.; Dietrich, A.; Goring, D. Effect of mercerization on the crystallite size and crystallinity index in cellulose from different sources. *Can. J. Chem.* **1987**, *65*, 1724–1725. [CrossRef]
11. Su, Y.; Burger, C.; Ma, H.; Chu, B.; Hsiao, B. Morphological and property investigations of carboxylated cellulose nanofibers extracted from different biological species. *Cellulose* **2015**, *22*, 3127–3135. [CrossRef]
12. Kargarzadeh, H.; Ahmad, I.; Abdullah, I.; Dufresne, A.; Zainudin, S.; Sheltami, R. Effects of hydrolysis conditions on the morphology, crystallinity, and thermal stability of cellulose nanocrystals extracted from kenaf bast fibers. *Cellulose* **2012**, *19*, 855–866. [CrossRef]
13. Krishnan, A.; Jose, C.; George, K. Sisal nanofibril reinforced polypropylene/polystyrene blends: Morphology, mechanical, dynamic mechanical and water transmission studies. *Ind. Crops Prod.* **2015**, *71*, 173–184. [CrossRef]
14. Ikkala, O.; Walther, A.; Ras, R.; Bergland, L.A. Native cellulose nanofibers: From biomimetic nanocomposites to functionalized gel spun fibers and functional aerogels. In *Abstracts of Papers of the American Chemical Society*, Proceedings of the 11th International Biorelated Polymer Symposium/243rd National Spring Meeting of the American-Chemical-Society (ACS), San Diego, CA, USA, 25–29 Marth 2012.
15. Saleh, M.H.S.D.E.; Muhamad, M.D.I.I.; Mamat, S.N.H. Cellulose Nanofiber Isolation and Its Fabrication into Bio-Polymer-A Review. In Proceedings of the International Conference on Agricultural and Food Engineering for Life (Cafei2012), Putrajaya, Malaysia, 26–28 November 2012; p. 28.
16. Maiti, S.; Jayaramudu, J.; Das, K.; Reddy, S.M.; Sadiku, R.; Ray, S.S.; Liu, D. Preparation and characterization of nano-cellulose with new shape from different precursor. *Carbohydr. Polym.* **2013**, *98*, 562–567. [CrossRef] [PubMed]
17. Hall, M.; Bansal, P.; Lee, J.H.; Realff, M.J.; Bommarius, A.S. Biological pretreatment of cellulose: Enhancing enzymatic hydrolysis rate using cellulose-binding domains from cellulases. *Bioresour. Technol.* **2011**, *102*, 2910–2915. [CrossRef] [PubMed]
18. Capitani, D.; Porro, F.; Segre, A. High field NMR analysis of the degree of substitution in carboxymethyl cellulose sodium salt. *Carbohydr. Polym.* **2000**, *42*, 283–286. [CrossRef]
19. Lai, Y.-Z. Wood and Wood Products. In *Handbook of Industrial Chemistry and Biotechnology*; Springer: Berlin, Germany; Heidelberg, Germany, 2012; pp. 1057–1115.

20. Oyourou, J.-N.; Combrinck, S.; Regnier, T.; Marston, A. Purification, stability and antifungal activity of verbascoside from Lippia javanica and Lantana camara leaf extracts. *Ind. Crops Prod.* **2013**, *43*, 820–826. [CrossRef]
21. Finkenstadt, V.L. A Review on the Complete Utilization of the Sugarbeet. *Sugar Tech* **2014**, *16*, 339–346. [CrossRef]
22. Haleem, N.; Arshad, M.; Shahid, M.; Tahir, M.A. Synthesis of carboxymethyl cellulose from waste of cotton ginning industry. *Carbohydr. Polym.* **2014**, *113*, 249–255. [CrossRef] [PubMed]
23. Heinze, T.; Liebert, T.; Klüfers, P.; Meister, F. Carboxymethylation of cellulose in unconventional media. *Cellulose* **1999**, *6*, 153–165. [CrossRef]
24. Biswas, A.; Kim, S.; Selling, G.W.; Cheng, H. Conversion of agricultural residues to carboxymethylcellulose and carboxymethylcellulose acetate. *Ind. Crops Prod.* **2014**, *60*, 259–265. [CrossRef]
25. Pushpamalar, V.; Langford, S.J.; Ahmad, M.; Hashim, K.; Lim, Y.Y. Preparation of carboxymethyl sago pulp hydrogel from sago waste by electron beam irradiation and swelling behavior in water and various pH media. *J. Appl. Polym. Sci.* **2013**, *128*, 451–459. [CrossRef]
26. Anastas, P.T.; Warner, J.C. *Green Chemistry: Theory and Practice*; Oxford University Press: New York, NY, USA, 2000.
27. Wenz, G.; Liepold, P.; Bordeanu, N. Synthesis and SAM formation of water soluble functional carboxymethylcelluloses: thiosulfates and thioethers. *Cellulose* **2005**, *12*, 85–96. [CrossRef]
28. Miranda, I.; Gominho, J.; Mirra, I.; Pereira, H. Fractioning and chemical characterization of barks of Betula pendula and Eucalyptus globulus. *Ind. Crops Prod.* **2013**, *41*, 299–305. [CrossRef]
29. He, Y.; Pang, Y.; Liu, Y.; Li, X.; Wang, K. Physicochemical characterization of rice straw pretreated with sodium hydroxide in the solid state for enhancing biogas production. *Energy Fuels* **2008**, *22*, 2775–2781. [CrossRef]
30. Pushpamalar, V.; Langford, S.; Ahmad, M.; Lim, Y.Y. Optimization of reaction conditions for preparing carboxymethyl cellulose from sago waste. *Carbohydr. Polym.* **2006**, *64*, 312–318. [CrossRef]
31. Zhou, J.; Zhang, L. Solubility of cellulose in NaOH/urea aqueous solution. *Polym. J.* **2000**, *32*, 866–870. [CrossRef]
32. Bao, D.; Chen, M.; Wang, H.; Wang, J.; Liu, C.; Sun, R. Preparation and characterization of double crosslinked hydrogel films from carboxymethylchitosan and carboxymethylcellulose. *Carbohydr. Polym.* **2014**, *110*, 113–120. [CrossRef] [PubMed]
33. Morán, J.I.; Alvarez, V.A.; Cyras, V.P.; Vázquez, A. Extraction of cellulose and preparation of nanocellulose from sisal fibers. *Cellulose* **2008**, *15*, 149–159. [CrossRef]
34. Mammino, L.; Kabanda, M.M. A study of the intramolecular hydrogen bond in acylphloroglucinols. *J. Mol. Struct. Theochem* **2009**, *901*, 210–219. [CrossRef]
35. Schulz, H.; Baranska, M. Identification and quantification of valuable plant substances by IR and Raman spectroscopy. *Vib. Spectrosc.* **2007**, *43*, 13–25. [CrossRef]
36. Wu, L.M.; Tong, D.S.; Zhao, L.Z.; Yu, W.H.; Zhou, C.H.; Wang, H. Fourier transform infrared spectroscopy analysis for hydrothermal transformation of microcrystalline cellulose on montmorillonite. *Appl. Clay Sci.* **2014**, *95*, 74–82. [CrossRef]
37. Singh, R.; Kant, K.; Mahto, V. Study of the Gelation and Rheological Behavior of Carboxymethyl Cellulose-Polyacrylamide Graft Copolymer Hydrogel. *J. Dispers. Sci. Technol.* **2015**, *36*, 877–884. [CrossRef]
38. Park, H.-R.; Ghafoor, K.; Lee, D.; Kim, S.; Kim, S.-H.; Park, J. β-Glycosidase-assisted bioconversion of ginsenosides in purified crude saponin and extracts from red ginseng (Panax ginseng C.A.Meyer). *Food Sci. Biotechnol.* **2013**, *22*, 1629–1638. [CrossRef]
39. Haafiz, M.M.; Hassan, A.; Zakaria, Z.; Inuwa, I. Isolation and characterization of cellulose nanowhiskers from oil palm biomass microcrystalline cellulose. *Carbohydr. Polym.* **2014**, *103*, 119–125. [CrossRef] [PubMed]
40. Haafiz, M.M.; Eichhorn, S.; Hassan, A.; Jawaid, M. Isolation and characterization of microcrystalline cellulose from oil palm biomass residue. *Carbohydr. Polym.* **2013**, *93*, 628–634. [CrossRef] [PubMed]
41. Huang, Y.-B.; Fu, Y. Hydrolysis of cellulose to glucose by solid acid catalysts. *Green Chem.* **2013**, *15*, 1095–1111. [CrossRef]
42. Koo, B.; Kim, H.; Cho, Y.; Lee, K.T.; Choi, N.S.; Cho, J. A Highly Cross-Linked Polymeric Binder for High-Performance Silicon Negative Electrodes in Lithium Ion Batteries. *Angew. Chem. Int. Ed.* **2012**, *51*, 8762–8767. [CrossRef] [PubMed]

43. Gašparovič, L.; Koreňová, Z.; Jelemenský, Ľ. Kinetic study of wood chips decomposition by TGA. *Chem. Pap.* **2010**, *64*, 174–181. [CrossRef]
44. Hamdaoui, L.; Moussaouiti, M.; Gmouh, S. Preparation and characterization of cellulose p-phenylbenzoate by two-step synthesis from microcrystalline and kraft cellulose. *Polym. Bull.* **2015**, *72*, 1–12. [CrossRef]
45. Barneto, A.; Vila, C.; Ariza, J.; Vidal, T. Thermogravimetric measurement of amorphous cellulose content in flax fibre and flax pulp. *Cellulose* **2011**, *18*, 17–31. [CrossRef]
46. Sen, U.K.; Mitra, S. High-rate and high-energy-density lithium-ion battery anode containing 2D MoS2 nanowall and cellulose binder. *ACS Appl. Mater. Interfaces* **2013**, *5*, 1240–1247. [CrossRef] [PubMed]
47. Paunonen, S. Strength and barrier enhancements of cellophane and cellulose derivative films: A review. *BioResources* **2013**, *8*, 3098–3121. [CrossRef]
48. Von Schantz, L.; Schagerlöf, H.; Karlsson, E.N.; Ohlin, M. Characterization of the substitution pattern of cellulose derivatives using carbohydrate-binding modules. *BMC Biotechnol.* **2014**, *14*, 113. [CrossRef] [PubMed]
49. Merkel, K.; Rydarowski, H.; Kazimierczak, J.; Bloda, A. Processing and characterization of reinforced polyethylene composites made with lignocellulosic fibres isolated from waste plant biomass such as hemp. *Compos. Part B Eng.* **2014**, *67*, 138–144. [CrossRef]
50. Zhuang, C.; Tao, F.; Cui, Y. Anti-degradation gelatin films crosslinked by active ester based on cellulose. *RSC Adv.* **2015**, *5*, 52183–52193. [CrossRef]
51. Neto, W.P.F.; Silvério, H.A.; Vieira, J.G.; da Costa e Silva Alves, H.; Pasquini, D.; de Assunção, R.M.N.; Dantas, N.O. Macromolecular Symposia. In *Preparation and Characterization of Nanocomposites of Carboxymethyl Cellulose Reinforced with Cellulose Nanocrystals*; Wiley Online Library: Weinheim, Germany, 2012; pp. 93–98.
52. Tzia, C.; Giannou, V.; Lebesi, D.; Cranioti, C. *Chemistry and Functional Properties of Carbohydrates and Sugars (Monosaccharides, Disaccharides, and Polysaccharides)*; CRC Press, Taylor & Francis Group: Park Drive, Abingdon, UK, 2012.
53. Lazik, W.; Heinze, T.; Pfeiffer, K.; Albrecht, G.; Mischnick, P. Starch derivatives of a high degree of functionalization. VI. Multistep carboxymethylation. *J. Appl. Polym. Sci.* **2002**, *86*, 743–752. [CrossRef]
54. Kono, H. Characterization and properties of carboxymethyl cellulose hydrogels crosslinked by polyethylene glycol. *Carbohydr. Polym.* **2014**, *106*, 84–93. [CrossRef] [PubMed]
55. Isogai, A.; Usuda, M.; Kato, T.; Uryu, T.; Atalla, R.H. Solid-state CP/MAS carbon-13 NMR study of cellulose polymorphs. *Macromolecules* **1989**, *22*, 3168–3172. [CrossRef]
56. Silva, L.S.; Lima, L.C.; Silva, F.C.; Matos, J.M.E.; Santos, M.R.M.; Júnior, L.S.S.; Sousa, K.S.; da Silva Filho, E.C. Dye anionic sorption in aqueous solution onto a cellulose surface chemically modified with aminoethanethiol. *Chem. Eng. J.* **2013**, *218*, 89–98. [CrossRef]
57. Balakshin, M.; Capanema, E.; Gracz, H.; Chang, H.-M.; Jameel, H. Quantification of lignin–carbohydrate linkages with high-resolution NMR spectroscopy. *Planta* **2011**, *233*, 1097–1110. [CrossRef] [PubMed]
58. Waring, M.; Parsons, D. Physico-chemical characterisation of carboxymethylated spun cellulose fibres. *Biomaterials* **2001**, *22*, 903–912. [CrossRef]
59. Heinze, T.; Koschella, A. Macromolecular Symposia. In *Carboxymethyl Ethers of Cellulose and starch–A Review*; Wiley Online Library: Weinheim, Germany, 2005; pp. 13–40.
60. Sheldon, R.A. Fundamentals of green chemistry: efficiency in reaction design. *Chem. Soc. Rev.* **2012**, *41*, 1437–1451. [CrossRef] [PubMed]
61. Adinugraha, M.P.; Marseno, D.W. Synthesis and characterization of sodium carboxymethylcellulose from cavendish banana pseudo stem (Musa cavendishii LAMBERT). *Carbohydr. Polym.* **2005**, *62*, 164–169. [CrossRef]
62. Nomura, H.; Koda, S.; Hattori, F. Viscosity of aqueous solutions of polysaccharides and their carboxylate derivatives. *J. Appl. Polym. Sci.* **1990**, *41*, 2959–2969. [CrossRef]
63. Dumitriu, S. Polysaccharides as biomaterials. *Polym. Biomater.* **2001**, *29*, 1–61.
64. Rando, R.F.; Obara, S.; Osterling, M.C.; Mankowski, M.; Miller, S.R.; Ferguson, M.L.; Krebs, F.C.; Wigdahl, B.; Labib, M.; Kokubo, H. Critical design features of phenyl carboxylate-containing polymer microbicides. *Antimicrob. Agents Chemother.* **2006**, *50*, 3081–3089. [CrossRef] [PubMed]